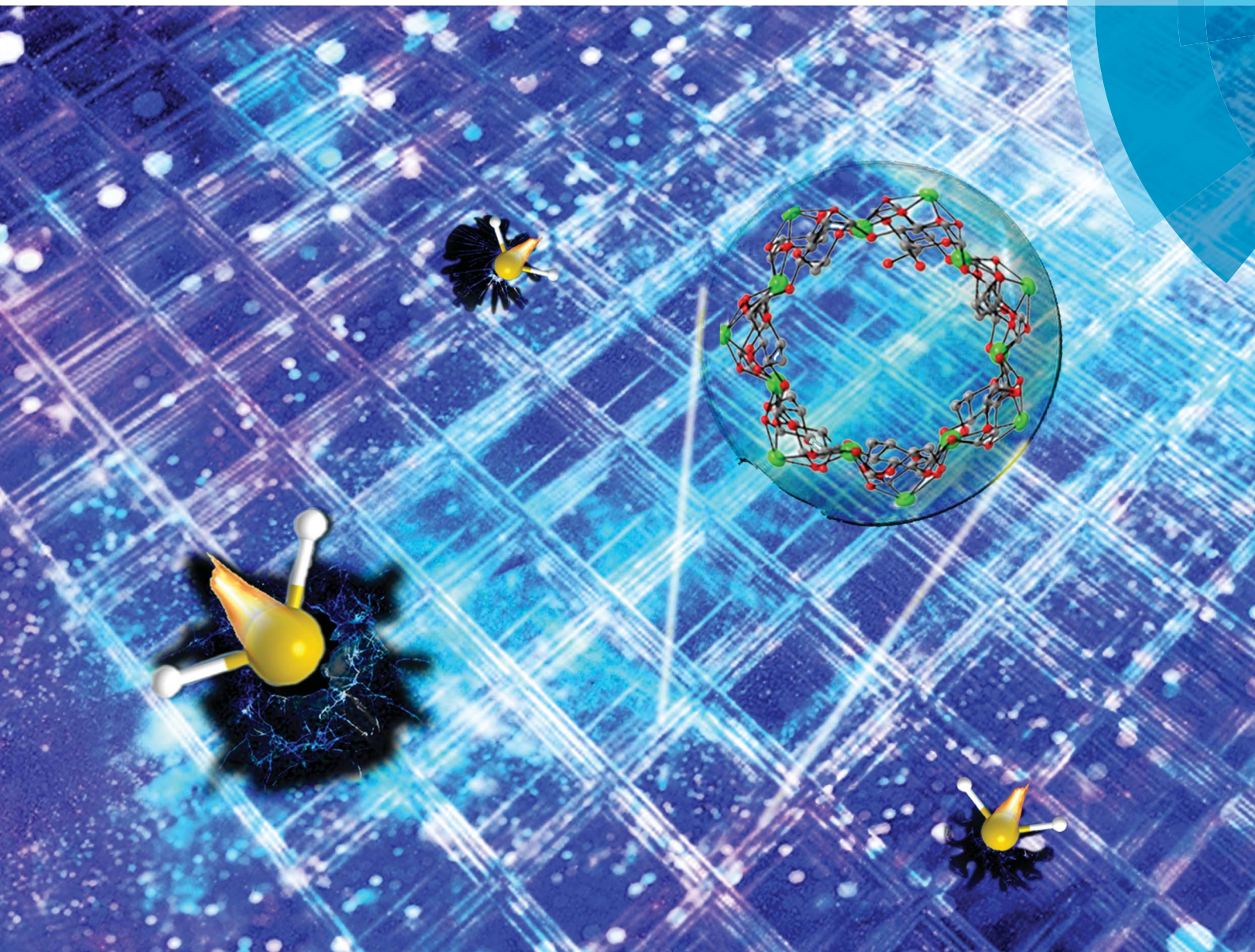


# Analytical Methods

rsc.li/methods



ISSN 1759-9679



**PAPER**

Fangna Dai, Rongming Wang, Daofeng Sun *et al.*  
A visual test paper based on Pb(II) metal–organic nanotubes utilized as a H<sub>2</sub>S sensor with high selectivity and sensitivity

Cite this: *Anal. Methods*, 2017, 9, 3094

# A visual test paper based on Pb(II) metal–organic nanotubes utilized as a H<sub>2</sub>S sensor with high selectivity and sensitivity†

Xuelian Xin, Fangna Dai,\* Fugang Li, Xin Jin, Rongming Wang\* and Daofeng Sun \*

The fluorescent Pb(II)–metal–organic nanotube, CD-MONT-2, which possesses a large {Pb<sub>14</sub>} metallamacrocycle, is synthesized by a modified biphasic liquid–solid–liquid (BLSL) strategy. This strategy takes advantage of solid cyclohexanol to avoid generation of by-products, and is suitable for producing CD-MONT-2 on a large scale. Importantly, water-stable CD-MONT-2 can be easily made into H<sub>2</sub>S test papers by coating a solution mixture of sodium carboxymethyl cellulose and CD-MONT-2' on glass plates, which have the characteristics of high efficiency, rapidity, and visualization based on its fluorescence “turn-off” response. The CD-MONT-2 based visual test papers can be used without pretreatment and possess excellent sensitivity and stability.

Received 9th March 2017

Accepted 4th April 2017

DOI: 10.1039/c7ay00627f

rsc.li/methods

## Introduction

Chemical sensors have been widely utilized in various fields, such as automation, safety, and the chemical industry. For different sensors, their sensing principles are versatile.<sup>1</sup> Recently, the sensors of metal–organic complexes with excellent fluorescence properties have attracted great attention owing to their excellent stability, outstanding selectivity, and enhanced sensitivity.<sup>2–6</sup> As a special type of metal–organic complexes, metal–organic nanotubes (MONTs), which are composed of metal ions and organic ligands, exhibit potential applications in gas adsorption and separation, luminescence detection, and catalysis.<sup>7–10</sup> Until recently, researchers have investigated their fluorescence sensing properties in detecting H<sub>2</sub>S. In 2014, Tang *et al.* reported a nanoscale metal–organic framework for H<sub>2</sub>S detection based on the fluorescence turn-on properties arising from the low-solubility of CuS precipitation ( $K_{sp} = 6.3 \times 10^{-36}$ ), which was successfully used in living cells. This work illustrated the great opportunity for the development of the crossover between metal–organic complexes and fluorescence techniques.<sup>11</sup>

Hydrogen sulfide (H<sub>2</sub>S), a toxic gas with a malodorous smell of rotten eggs, has been known as an inflammable and explosive industrial pollutant for many years.<sup>12–16</sup> Even a low concentration of H<sub>2</sub>S in the open air leads to metallic corrosion and is a serious detriment to human health.<sup>2</sup> Currently, the common methods for H<sub>2</sub>S detection are colorimetric determination, gas

chromatography, electrochemical assays, and sulfide precipitation.<sup>17–21</sup> Lead acetate (PbAc<sub>2</sub>) test papers are widely used for H<sub>2</sub>S detection due to their simplicity and fast response. However, PbAc<sub>2</sub> papers are susceptible to deterioration in air to form PbCO<sub>3</sub> (PbAc<sub>2</sub>·3H<sub>2</sub>O + CO<sub>2</sub> = PbCO<sub>3</sub> + 3H<sub>2</sub>O + 2HAc), leading to poor durability.<sup>22</sup> As an easy and practical technique, fluorescence-based assay shows excellent application in the detection of H<sub>2</sub>S because of its non-destructive feature, high sensitivity, and convenience.<sup>23–25</sup> The reported fluorescent sensors for H<sub>2</sub>S detection are mostly based on the following mechanisms: (a) reduction of azide or nitro groups, (b) reactions of nucleophilic addition and Michael addition, (c) oxidation–reduction reactions of versatile selenium, and (d) quencher (such as Ag<sup>+</sup>, Pb<sup>2+</sup>, Cu<sup>2+</sup> and Hg<sup>2+</sup> ions) removal.<sup>26,27</sup>

Herein, we report visual test papers based on water-stable Pb(II)–MONTs (CD-MONT-2, which possesses a large {Pb<sub>14</sub>} metallamacrocycle,<sup>28</sup> reported in 2012). The CD-MONT-2 is utilized as a H<sub>2</sub>S sensor with good selectivity and sensitivity. The CD-MONT-2 is synthesized by a modified strategy with higher yield and improved crystallinity. Importantly, the aqueous solution of CD-MONT-2 and sodium carboxymethyl cellulose (CMC) can be simply spread on glass plates to prepare test papers,<sup>29</sup> which have the ability of rapid and visual detection of H<sub>2</sub>S with both efficiency and accuracy.

## Experimental

### Physical measurements and fluorescence experiments

Fluorescence (FL) spectra were recorded on a Hitachi F-7000 fluorescence spectrophotometer. Samples were excited at 330 nm with the excitation and emission slit widths of 20 and 20 nm, respectively. The emission spectra were scanned from 350 to 700 nm at 1200 nm min<sup>-1</sup>. The photomultiplier voltage

State Key Laboratory of Heavy Oil Processing, College of Science, China University of Petroleum (East China), Qingdao, Shandong 266580, China. E-mail: dfsun@upc.edu.cn; rmwang@upc.edu.cn; fndai@upc.edu.cn

† Electronic supplementary information (ESI) available: Structure of CD-MONT-2, materials and methods, PXRD data, fluorescence spectra, XPS spectra, FTIR spectra and TEM image. See DOI: 10.1039/c7ay00627f



was set at 400 V. Powder X-ray diffraction (PXRD) data are obtained on a Philips X' Pert with Cu-K $\alpha$  radiation ( $\lambda = 0.15418$  nm). Fourier transform infrared spectroscopy (FTIR) spectra were collected on a Bruker VERTEX-70 spectrometer in the 4000–600  $\text{cm}^{-1}$  region. The morphology and structure of the prepared samples were observed by scanning electron microscopy (SEM, JSM-7500F) and transmission electron microscopy (TEM, Tecnai-G20) with an accelerating voltage of 200 kV, respectively. The X-ray photoelectron spectra (XPS) were obtained with a Thermo Scientific (USA) K-Alpha electron spectrometer with Al-K $\alpha$  ( $h\nu = 1486.6$  eV) radiation. The experimental materials are shown in S1, ESI†

### A modified biphasic liquid–solid–liquid (BLSL) synthesis

The synthesis of metal–organic materials containing Pb(II), Cu(II) and Fe(III) in alkaline systems remains very difficult because of the formation of precipitates of  $\text{Pb}(\text{OH})_2$ ,  $\text{Cu}(\text{OH})_2$ , and  $\text{Fe}(\text{OH})_3$ .<sup>9</sup> Although the import of the biphasic method (two immiscible liquids) partly solved the issues, the wavy and unstable nature of liquids tremendously hinders high-yield and large scale synthesis.<sup>30,31</sup> Based on the previously reported method,<sup>28</sup> colourless crystals of **CD-MONT-2** are obtained. In this reaction, cyclohexanol is used as a block to slow down the diffusion rate of triethylamine, which can prevent the formation of by-products. When repeated trials were conducted by using small vials with a diameter of 1.6 centimeter, we found that the product seems to have better crystallinity and higher yield at a lower room temperature. We suggest that it results from the slower diffusion rate of triethylamine due to the solidification of cyclohexanol below 25.93 °C. Hence, we attempted a modified method, “biphasic liquid–solid–liquid (BLSL)” synthesis (Fig. 1). After the cyclohexanol was layered onto the H<sub>2</sub>O phase with  $\text{PbCl}_2$  and  $\beta$ -CD, the vials were kept at 4 °C and then the triethylamine was layered onto the cyclohexanol solids. The details of the procedure to synthesize **CD-MONT-2** are described in S2, ESI† The obtained crystals' structure was confirmed to be the same as the reported one.<sup>28</sup> Compared with the reported biphasic synthesis,<sup>28</sup> solidified cyclohexanol makes the addition of triethylamine easier, and limits the diffusion of alkaline triethylamine to the bottom

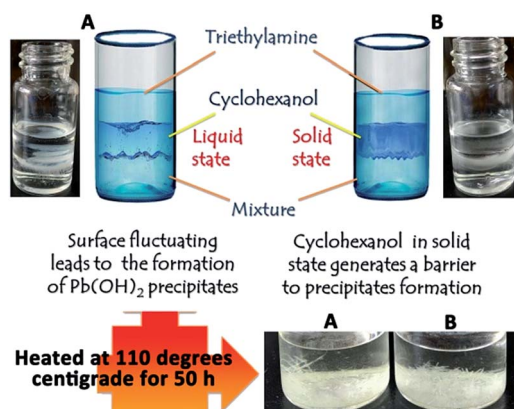


Fig. 1 (A) Original synthesis of amplification; (B) BLSL synthesis of amplification.

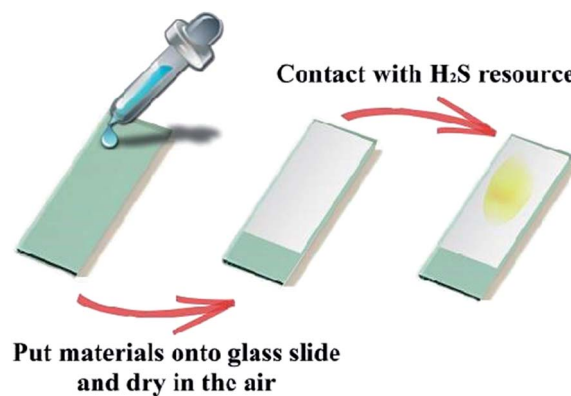


Fig. 2 The preparation and H<sub>2</sub>S detection of test papers.

solution which reduces the metal hydroxide by-products to a large extent. Subsequently, the vials were sealed and heated at 110 °C for 50 hours to produce **CD-MONT-2** crystals with a higher yield (*ca.* 89%, mean of three replicates) and better crystallinity (Fig. 1) in comparison to the previous report (*ca.* 65%, mean of three replicates). According to the obtained structure, the dimension of cavities in **CD-MONT-2** is *ca.* 13.0 × 10.3 × 10.2 Å with cyclohexanol molecules filling inside. The guest cyclohexanol molecules are removed by heating at 120 °C for 1 hour to obtain the guest-free form, **CD-MONT-2'**. The phase purity of the bulk product is confirmed by matching the PXRD pattern of the as-synthesized bulk complex with that of the simulated one from single-crystal data, and the structural integrity of the activated **CD-MONT-2'** obtained by the BLSL synthetic method is also confirmed by matching PXRD patterns (Fig. S1, ESI†). Obviously, the features of high yield and simple operation of the BLSL method indicate that it is more suitable for production on a large scale.

### Preparation of test papers

**CD-MONT-2'** shows excellent dispersion and stability in H<sub>2</sub>O, and the method of silica gel plate preparation is used to obtain a test paper. 100 mg powder of **CD-MONT-2'** were ground and added into 10 mL 0.5% aqueous CMC to obtain a homogeneous suspension by ultrasonication for one hour, and then the resultant suspension was spread on clean glass plates (1.5 × 3.5 cm<sup>2</sup>) and dried overnight in the air (Fig. 2). The test papers are confirmed by matching the PXRD pattern of the as-made test papers, a simulated one from single-crystal data, and the structural integrity of the activated **CD-MONT-2'** (Fig. S2, ESI†).

## Results and discussion

### Sensing behavior of **CD-MONT-2'**

Crystals of **CD-MONT-2'** were ground and added into H<sub>2</sub>O (1 mg mL<sup>-1</sup>) to form a homogeneous suspension under ultrasonic vibration for an hour.<sup>32</sup> Then, fluorescence tests were performed by gradually adding Na<sub>2</sub>S aqueous solution (as a H<sub>2</sub>S source) to the aforementioned suspension with fluorescence emission at 432 nm upon excitation at 330 nm. Accompanying gradual

addition of  $\text{Na}_2\text{S}$  solution ( $1 \text{ mmol L}^{-1}$ ), the fluorescence intensities significantly drop, implying the obvious response to the  $\text{H}_2\text{S}$  source (Fig. 3a and the inset picture). When the concentration of  $\text{Na}_2\text{S}$  increases to the range between  $100 \mu\text{M}$  and  $200 \mu\text{M}$ , the fluorescence intensity of **CD-MONT-2'** remains unchanged, suggesting that the sensor is saturated.

The fluorescence intensities show an excellent linear response to  $\text{Na}_2\text{S}$  concentrations between  $1 \mu\text{M}$  and  $6 \mu\text{M}$ , as illustrated in the inset picture of Fig. 3b (where  $I_0$  is the initial fluorescence intensity and  $I$  is the fluorescence intensity after addition of  $\text{Na}_2\text{S}$  solution, and the decrease of fluorescence intensities with gradual increment of  $\text{Na}_2\text{S}$  is shown in Fig. S3†). The limit of detection (LOD) can be calculated by using the following equation:  $\text{LOD} = k \times \sigma/S$ , where the  $k$  value is 3 (repeated times),  $\sigma$  value is 25.73 (calculated from 11 groups of blank test) and  $S$  value is 99.32 (based on the linear regression). It is worth noting that the probe is highly sensitive to a low concentration of  $\text{S}^{2-}$ , and the detection limit for  $\text{S}^{2-}$  is estimated to be  $0.78 \mu\text{M}$ .

To evaluate the specific nature of **CD-MONT-2'** for  $\text{H}_2\text{S}$ , the fluorescence titrations of aqueous solutions of other substances

including salts ( $\text{Na}_2\text{SO}_4$ ,  $\text{Na}_2\text{SO}_3$ ,  $\text{Na}_2\text{CO}_3$ ,  $\text{NaCl}$ ,  $\text{NaClO}$ ,  $\text{NaAc}$ ,  $\text{NaH}_2\text{PO}_4$ ,  $\text{KCl}$ ,  $\text{KI}$  and  $\text{KBr}$ ), sulphur compounds ( $\text{GSH}$ ,  $\text{l-cys}$  and  $\text{THU}$ ), reducing agents (glucose), non-thiol amino acids ( $\text{Gln}$  and  $\text{DL-Tyr}$ ), and reactive oxygen species ( $\text{H}_2\text{O}_2$  and  $^t\text{BuOOH}$ )<sup>33–35</sup> were also carried out as the same procedure with  $\text{Na}_2\text{S}$ , the full spectra are shown in Fig. S4, ESI.† The fluorescence intensities of  $I_0/I$  spectra ( $\lambda = 432 \text{ nm}$ ) are presented in Fig. 3b and S5.† The results suggest that **CD-MONT-2'** possesses high selectivity and sensitivity to  $\text{H}_2\text{S}$  sources attributed to its remarkable fluorescence “turn-off” response.

### Sensitivity and characterization of test papers

To explore the sensing properties of **CD-MONT-2'**-based  $\text{H}_2\text{S}$  test papers, a test paper was put  $0.5 \text{ cm}$  over the top of the flask ( $150 \text{ mL}$ ) filled with  $\text{H}_2\text{S}$ . Compared with a blank test paper, the one in contact with  $\text{H}_2\text{S}$  turned brown, and no fluorescence was observed under the UV lamp of  $365 \text{ nm}$  within  $90 \text{ s}$ . From the SEM images of test papers before and after being treated with  $\text{H}_2\text{S}$  (Fig. 4), we can clearly observe the crystals of **CD-MONT-2'** before detection (Fig. 4a and b) and non-crystalline substances after coming in contact with  $\text{H}_2\text{S}$  (Fig. 4c and d), indicating the

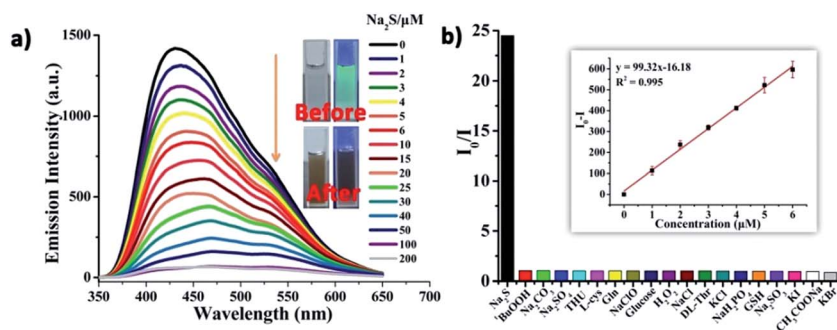


Fig. 3 (a) FL spectra of  $1 \text{ mg mL}^{-1}$  **CD-MONT-2'** in  $\text{H}_2\text{O}$  treated with the addition of different quantities of  $\text{Na}_2\text{S}$ , and the inset pictures are **CD-MONT-2'** suspensions without and with the irradiation of a UV lamp. (b) The relative fluorescence intensity  $I_0/I$  at  $432 \text{ nm}$  with  $100 \mu\text{M}$  of  $\text{Na}_2\text{S}$ , inorganic salts, reducing agents, amino acids and ROS, and the inset picture is the excellent linear response of the fluorescence intensity.

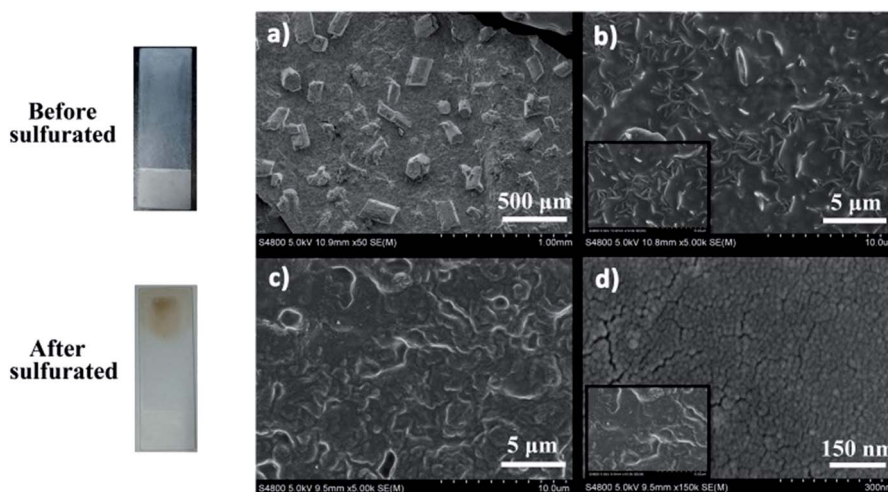


Fig. 4 SEM micrographs of **CD-MONT-2'** test papers before (a) and (b) and after (c) and (d) being treated with a continuous supply of  $\text{H}_2\text{S}$  for  $90 \text{ s}$ .

inexistence of **CD-MONT-2'**. In addition, compared with lead acetate test papers, the **CD-MONT-2'** test papers show a more evident color change within 10 min when coming in contact with the same concentration of  $\text{Na}_2\text{S}$  solutions. The evident color of **CD-MONT-2'** test papers remains unchanged for more than 30 min after the test, while the lead acetate test papers are almost blank (Fig. 5). Therefore, the **CD-MONT-2'** test paper possesses better sensitivity and long-lasting stability when comparing with the lead acetate paper.

To explore the detection mechanism of **CD-MONT-2'** towards  $\text{H}_2\text{S}$ , FL, PXRD, XPS, FTIR, and TEM tests are carried out for the solid samples of **CD-MONT-2'** before and after being treated with  $\text{H}_2\text{S}$  (**CD-MONT-2'**-derivatives). The remarkable fluorescence "turn-off" response of **CD-MONT-2'** to  $\text{H}_2\text{S}$  (Fig. 6a) is due to the formation of lead-containing brown compounds containing  $\text{Pb}_4\text{-SO}_4(\text{CO}_3)_2(\text{OH})_2$ ,  $\text{PbCO}_3$ ,  $\text{PbSO}_3$  and  $\text{PbS}$  after coming in contact with  $\text{H}_2\text{S}$  in air, as confirmed by the PXRD results (Fig. 6b). The XPS survey scan spectra of Pb of **CD-MONT-2'**-derivatives clearly display the peaks of Pb  $4f_{7/2}$  with binding energies of 137.7 and 138.6 eV, and the peaks of Pb  $4f_{5/2}$  with binding energies of 142.6 and 143.6 eV (Fig. 6c), which agree well with the values reported for Pb-O and Pb-S bonds, respectively. The spin-orbit splitting is 5.0 eV and 4.9 eV for Pb-O and Pb-S bonds, respectively. Compared with the spectrum of **CD-MONT-2'**, the peaks of Pb-S bonds became the main part in the spectrum of **CD-MONT-2'**-derivatives. Fig. 6d shows the XPS survey scan spectra of S of **CD-MONT-2'**-derivatives. The peaks at 162.0 eV (S  $2p_{1/2}$ ) and 160.8 eV (S  $2p_{3/2}$ ) match well with  $\text{S}^{2-}$ .<sup>36-38</sup> Other XPS spectra of Pb, C and O of **CD-MONT-2'** and **CD-MONT-2'**-derivatives are shown in Fig. S6, ESI.† Compared with **CD-MONT-2'**, there are several new peaks in the spectra of C 1s and O 1s of **CD-MONT-2'**-derivatives. The peaks with binding energies of 286.4 and 286.1 eV are assigned to the S-C bond, and the one with a binding energy of

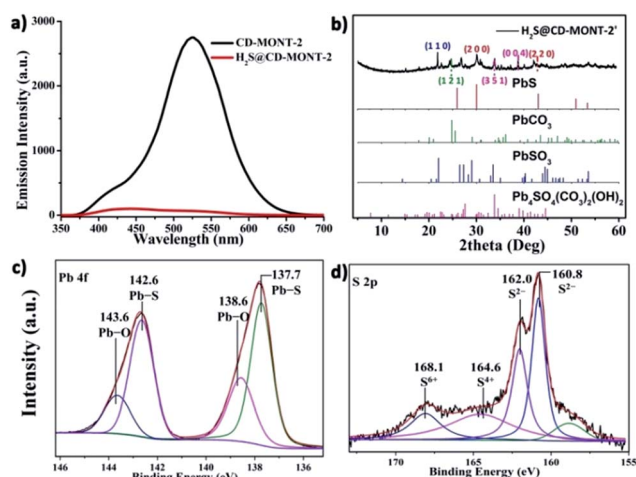


Fig. 6 FL spectra of **CD-MONT-2'** and **CD-MONT-2'**-derivatives (a); PXRD spectra of **CD-MONT-2'** derivatives (b); and XPS spectra of  $\text{Pb}_{4f}$  (c) and  $\text{S}_{2p}$  (d) of **CD-MONT-2'** derivatives.

532.2 eV is attributed to the S-O bond.<sup>39,40</sup> Moreover, the FTIR spectra of **CD-MONT-2'** and **CD-MONT-2'**-derivatives are shown in Fig. S7.† The spectrum of **CD-MONT-2'**-derivatives shows absorption bands around 3391, 2924, 1634, 1027 and 855  $\text{cm}^{-1}$ , among which the broad band around 3391  $\text{cm}^{-1}$  can be assigned to the bending vibrations of adsorbed water molecules and the stretching vibrations of hydroxyl groups. The peak around 1634  $\text{cm}^{-1}$  is attributed to the O-H bending vibrations of adsorbed water and hydroxyl groups,<sup>41</sup> and the peak around 1027  $\text{cm}^{-1}$  is ascribed to the stretching vibrations of C-O-C and C-O bonds. The new broad peaks around 1368  $\text{cm}^{-1}$  and 1108  $\text{cm}^{-1}$  originate from  $\text{CO}_3^{2-}$  and Pb-S bonds, respectively.<sup>42</sup> The TEM images provide more details about the structural evolution (Fig. S8, ESI†). The low-magnification TEM images show that the **CD-MONT-2'**-derivatives are splotchy and poly-crystallized, and the corresponding SAED (selected area electron diffraction) pattern indicates the non-crystalline feature of the brown compounds.<sup>43</sup> These results further demonstrate that the ability of **CD-MONT-2'** as a  $\text{H}_2\text{S}$  sensor arises from the transformation of **CD-MONT-2'** to inorganic substances.

## Conclusions

In summary, we report a modified biphasic liquid-solid-liquid (BLSL) strategy to prepare  $\text{Pb(II)}$ -MONTs of **CD-MONT-2'**, which presents an evident fluorescence "turn-off" response to  $\text{H}_2\text{S}$ . The BLSL strategy is an improvement to biphasic synthesis which provides a higher yield and is significantly applicable to the large-scale production of metal-organic complexes. Moreover, **CD-MONT-2'** can be utilized for fabricating visual  $\text{H}_2\text{S}$  test papers by smearing it on glass plates with a water solution of sodium carboxymethyl cellulose, and the test papers possess good selectivity and sensitivity to  $\text{H}_2\text{S}$  sources. The **CD-MONT-2'** visual test papers are easy to use and have good stability and sensitivity. We suggest that the remarkable fluorescence "turn-off" response originates from the decomposition of **CD-MONT-2'** into fluorescence silent species.

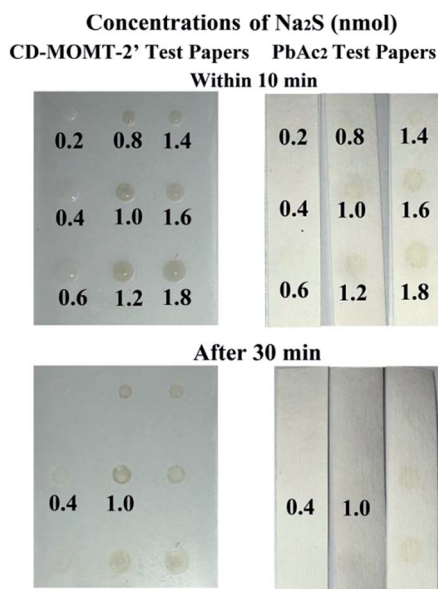


Fig. 5 The color change photos of **CD-MONT-2'** and lead acetate test papers treated with different concentrations of  $\text{Na}_2\text{S}$  within 10 min and after 30 min.



## Acknowledgements

This work was supported by the NSFC (Grant No. 21201179, 21371179, and 21571187), NCET-11-0309, Taishan Scholar Foundation (ts201511019), the Fundamental Research Funds for the Central Universities (16CX05015A) and the Applied Basic Research Projects of Qingdao (16-5-1-95-jch).

## Notes and references

- Z. Liang, T. H. Tsoi, C. F. Chan, L. Dai, Y. Wu, G. Du, L. Zhu, C. S. Lee, W. T. Wong, G. L. Law and K. L. Wong, *Chem. Sci.*, 2016, **7**, 2151.
- P. Horcajada, R. Gref, T. Baati, P. K. Allan, G. Maurin, P. Couvreur, G. Ferey, R. E. Morris and C. Serre, *Chem. Rev.*, 2012, **112**, 1232.
- O. Yassine, O. Shekhah, A. H. Assen, Y. Belmabkhout, K. N. Salama and M. Eddaoudi, *Angew. Chem., Int. Ed.*, 2016, **55**, 15879.
- A. M. Ebrahim, J. Jagiello and T. J. Bandosz, *J. Mater. Chem. A*, 2015, **3**, 8194.
- X. Zhou, S. Lee, Z. Xu and J. Yoon, *Chem. Rev.*, 2015, **115**, 7944.
- D. Fu, C. Zhu, X. Zhang, C. Li and Y. Chen, *J. Mater. Chem. A*, 2016, **4**, 1390.
- J. Lin, Q. Zhang, L. Wang, X. Liu, W. Yan, T. Wu, X. Bu and P. Feng, *J. Am. Chem. Soc.*, 2014, **136**, 4769.
- Q. Lin, X. Bu, C. Mao, X. Zhao, K. Sasan and P. Feng, *J. Am. Chem. Soc.*, 2015, **137**, 6184.
- M. Zhang, G. Feng, Z. Song, Y. P. Zhou, H. Y. Chao, D. Yuan, T. T. Tan, Z. Guo, Z. Hu, B. Z. Tang, B. Liu and D. Zhao, *J. Am. Chem. Soc.*, 2014, **136**, 7241.
- A. P. Jarosz, T. Yep and B. Mutus, *Anal. Chem.*, 2013, **85**, 3638.
- Y. W. Yip, G. L. Law and W. T. Wong, *Dalton Trans.*, 2016, **45**, 928.
- A. R. Lippert, E. J. New and C. J. Chang, *J. Am. Chem. Soc.*, 2011, **133**, 10078.
- L. Yin, D. Chen, M. Hu, H. Shi, D. Yang, B. Fan, G. Shao, R. Zhang and G. Shao, *J. Mater. Chem. A*, 2014, **2**, 18867.
- H. Huang, P. Xu, D. Zheng, C. Chen and X. Li, *J. Mater. Chem. A*, 2015, **3**, 6330.
- Z. Yuan, F. Lu, M. Peng, C. W. Wang, Y. T. Tseng, Y. Du, N. Cai, C. W. Lien, H. T. Chang, Y. He and E. S. Yeung, *Anal. Chem.*, 2015, **87**, 7267.
- Z. Zhang, Z. Chen, S. Wang, C. Qu and L. Chen, *ACS Appl. Mater. Interfaces*, 2014, **6**, 6300.
- M. D. Hartle and M. D. Pluth, *Chem. Soc. Rev.*, 2016, **44**, 4596.
- C. Liu, J. Pan, S. Li, Y. Zhao, L. Y. Wu, C. E. Berkman, A. R. Whorton and M. Xian, *Angew. Chem., Int. Ed.*, 2011, **50**, 10327.
- V. S. Lin, W. Chen, M. Xian and C. J. Chang, *Chem. Soc. Rev.*, 2015, **44**, 4596.
- H. Wu, Z. Chen, J. Zhang, F. Wu, C. He, B. Wang, Y. Wu and Z. Ren, *J. Mater. Chem. A*, 2016, **4**, 1096.
- N. Yu, H. Peng, H. Xiong, X. Wu, X. Wang, Y. Li and L. Chen, *Microchim. Acta*, 2015, **182**, 2139.
- G. L. Miessler, *et al.*, *Inorganic Chemistry*, Prentice Hall, 5th edn, vol. 7, 2013.
- Y. Pan, L. Ye and Z. Yuan, *Environ. Sci. Technol.*, 2013, **47**, 8408.
- J. Zhang and W. Guo, *Chem. Commun.*, 2014, **50**, 4214.
- S. Li, K. Yang, C. Tan, X. Huang, W. Huang and H. Zhang, *Chem. Commun.*, 2016, **52**, 1555.
- X. Wang, J. Sun, W. Zhang, X. Ma, J. Lv and B. Tang, *Chem. Sci.*, 2013, **4**, 2551.
- Y. Ma, H. Su, X. Kuang, X. Y. Li, T. T. Zhang and B. Tang, *Anal. Chem.*, 2014, **86**, 11459.
- Y. Wei, D. Sun, D. Yuan, Y. Liu, Y. Zhao, X. Li, S. Wang, J. Dou, X. Wang, A. Hao and D. Sun, *Chem. Sci.*, 2012, **3**, 2282.
- Z. Chen, Y. Sun, L. Zhang, D. Sun, F. Liu, Q. Meng, R. Wang and D. Sun, *Chem. Commun.*, 2013, **49**, 11557.
- A. Klinkova, E. M. Larin, E. Prince, E. H. Sargent and E. Kumacheva, *Chem. Mater.*, 2016, **28**, 3196.
- M. He, P. Huang, C. Zhang, H. Hu, C. Bao, G. Gao, R. He and D. Cui, *Adv. Funct. Mater.*, 2011, **21**, 4470.
- Z. Hu, W. P. Lustig, J. Zhang, C. Zheng, H. Wang, S. J. Teat, Q. Gong, N. D. Rudd and J. Li, *J. Am. Chem. Soc.*, 2015, **137**, 16209.
- J. Liu, K. K. Yee, K. K. Lo, K. Y. Zhang, W. P. To, C. M. Che and Z. Xu, *J. Am. Chem. Soc.*, 2014, **136**, 2818.
- X. Feng, T. Zhang, J. T. Liu, J. Y. Miao and B. X. Zhao, *Chem. Commun.*, 2016, **52**, 3131.
- L. Jin, H. Zhao, D. Ma, A. Vomiero and F. Rosei, *J. Mater. Chem. A*, 2015, **3**, 847.
- M. Guozheng, X. Binshi, W. Haidou, C. Shuying and X. Zhiguo, *ACS Appl. Mater. Interfaces*, 2014, **6**, 532.
- Y. Dong, J. Wen, F. Pang, Z. Chen, J. Wang, Y. Luo, G. Peng and T. Wang, *Appl. Surf. Sci.*, 2014, **320**, 372.
- D. J. Cant, K. L. Syres, P. J. Lunt, H. Radtke, J. Treacy, P. J. Thomas, E. A. Lewis, S. J. Haigh, P. O'Brien, K. Schulte, F. Bondino, E. Magnano and W. R. Flavell, *Langmuir*, 2015, **31**, 1445.
- J. Patel, F. Mighri, A. Ajji, D. Tiwari and T. K. Chaudhuri, *Appl. Phys. A*, 2014, **117**, 1791.
- W. M. Skinner, G. Qian and A. N. Buckley, *J. Solid State Chem.*, 2013, **206**, 32.
- Y. Huang, S. Li, H. Lin and J. Chen, *Appl. Surf. Sci.*, 2014, **317**, 422.
- C. Yuan, Z. Jin and X. Xu, *Carbohydr. Polym.*, 2012, **89**, 492.
- C. Zong, X. Liu, H. Sun, G. Zhang and L. Lu, *J. Mater. Chem.*, 2012, **22**, 18418.